Stress Intensity Formulas for Three-dimensional Cracks in the Vicinity of an Interface

著者	Noda Nao-Aki, Liang Bin
journal or publication title	Journal of Testing and Evaluation
volume	35
number	2
page range	192-202
year	2007-03-01
URL	http://hdl.handle.net/10228/00006132

doi: info:doi/10.1520/JTE100588

Journal of Testing and Evaluation, Vol. 35, No. 2
Paper ID JTE100588
Available online at: www.astm.org

Nao-Aki Noda[1] *and Bin Liang*[2]

Stress Intensity Formulas for Three-dimensional Cracks in the Vicinity of an Interface

ABSTRACT: In this study, stress intensity formulas are considered in terms of the square root of *area* parameter to evaluate arbitrary shaped defects or cracks in the vicinity of an interface. Here "area" is the projected area of the defect or crack. Stress intensity factors for an elliptical crack parallel to a bimaterial interface are considered with varying the distance, aspect ratio of the crack, and combinations of material's elastic constants. Also, stress intensity factors of an interface crack and a crack in a functionally graded material are investigated. Then, it is found that the maximum stress intensity factors normalized by the square root of *area* are always insensitive to the crack aspect ratio. They are given in a form of formulas useful for engineering applications.

KEYWORDS: fracture mechanics, stress intensity factor, bimaterial interface, crack

Nomenclature

a, b = dimensions of elliptical and rectangular cracks
a/b = aspect ratio of arbitrarily-shaped cracks assuming elliptical or rectangular approximation (see Fig. 1)
area = projected area of the crack or defects
h = distance from the crack to the interface (see Fig. 2)
G = $G=\mu_2/\mu_1$ when $0.3 \leqslant \mu_2/\mu_1 \leqslant 1.0$, or
G = $2-\mu_1/\mu_2$ when $1.0 \leqslant \mu_2/\mu_1 \leqslant \infty$ under normal loads
G = μ_2/μ_1 when $0.0 \leqslant \mu_2/\mu_1 \leqslant 1.0$, or
G = $2-\mu_1/\mu_2$ when $1.0 \leqslant \mu_2/\mu_1 \leqslant \infty$ under shear loads
H = $h/2b$
F_{i-n} $(i=I, II, III)$ = dimensionless stress intensity factors normalized by two-dimensional results under tension
F_{i-s} $(i=I, II, III)$ = dimensionless stress intensity factors normalized by two-dimensional results under shear
F^*_{i-n} $(i=I, II, III)$ = dimensionless factors normalized by $\sqrt{area}$ parameter under tension
F^*_{i-s} $(i=I, II, III)$ = dimensionless factors normalized by $\sqrt{area}$ parameter under shear
α = nonhomogeneity parameter for functionally graded materials
μ_1 = shear modulus for space 1
μ_2 = shear modulus for space 2
μ_2/μ_1 = shear modulus ratio
μ_0 = shear modulus of functionally graded materials at $z=0$
ν_1 = Poisson's ratio for space 1
ν_2 = Poisson's ratio for space 2

Manuscript received April 13, 2006; accepted for publication June 22, 2006; published online August 2006.

[1]Department of Mechanical Engineering, Kyushu Institute of Technology, 1-1 Sensui-cho Tobata, Kitakyushu 804-8550, Japan, E-mail: noda@mech.kyutech.ac.jp
[2]Department of Architectural Engineering, Henan University of Science and Technology, Xiyuan Road, Luoyang 471003, P. R. China.

Introduction

Since almost all structural materials contain some types of defects in the form of cracks, cavities, and inclusions, three-dimensional crack solutions may be useful for evaluating the strength of structures. In the previous studies, stress intensity formulas were proposed for evaluating the maximum stress intensity factors for arbitrary-shaped internal cracks subjected to tension σ_z^∞ and shear τ_{yz}^∞ at infinity for the coordinate system in Fig. 1 [1–6].

1. For the cracks subjected to tension σ_z^∞ [1,2]:

$$K_{\mathrm{Imax}} = 0.50\sigma_z^\infty \sqrt{\pi\sqrt{area}} \quad (1)$$

2. For the cracks subjected to shear τ_{yz}^∞ [3–6]:

$$K_{\mathrm{IImax}} = 0.55\tau_{yz}^\infty \sqrt{\pi\sqrt{area}} \quad (a/b \geqslant 1 \text{ in Fig. 1}) \quad (2)$$

$$K_{\mathrm{IIImax}} = 0.45\tau_{yz}^\infty \sqrt{\pi\sqrt{area}} \quad (a/b \leqslant 1 \text{ in Fig. 1}) \quad (3)$$

where "*area*" is the projected area of the crack or defects. For example, in Fig. 1(*a*), $area=\pi ab$, and in Fig. 1(*b*) $area=4ab$. However, it should be noted that $area=20b^2$ when $a/b \geqslant 5$, and $area=20a^2$ when $a/b \leqslant 0.2$ [1,2].

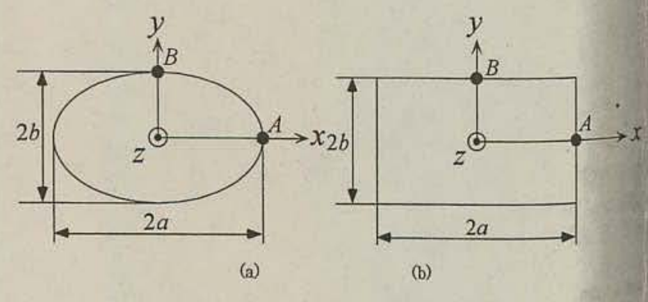

FIG. 1—*An elliptical and rectangular crack.*

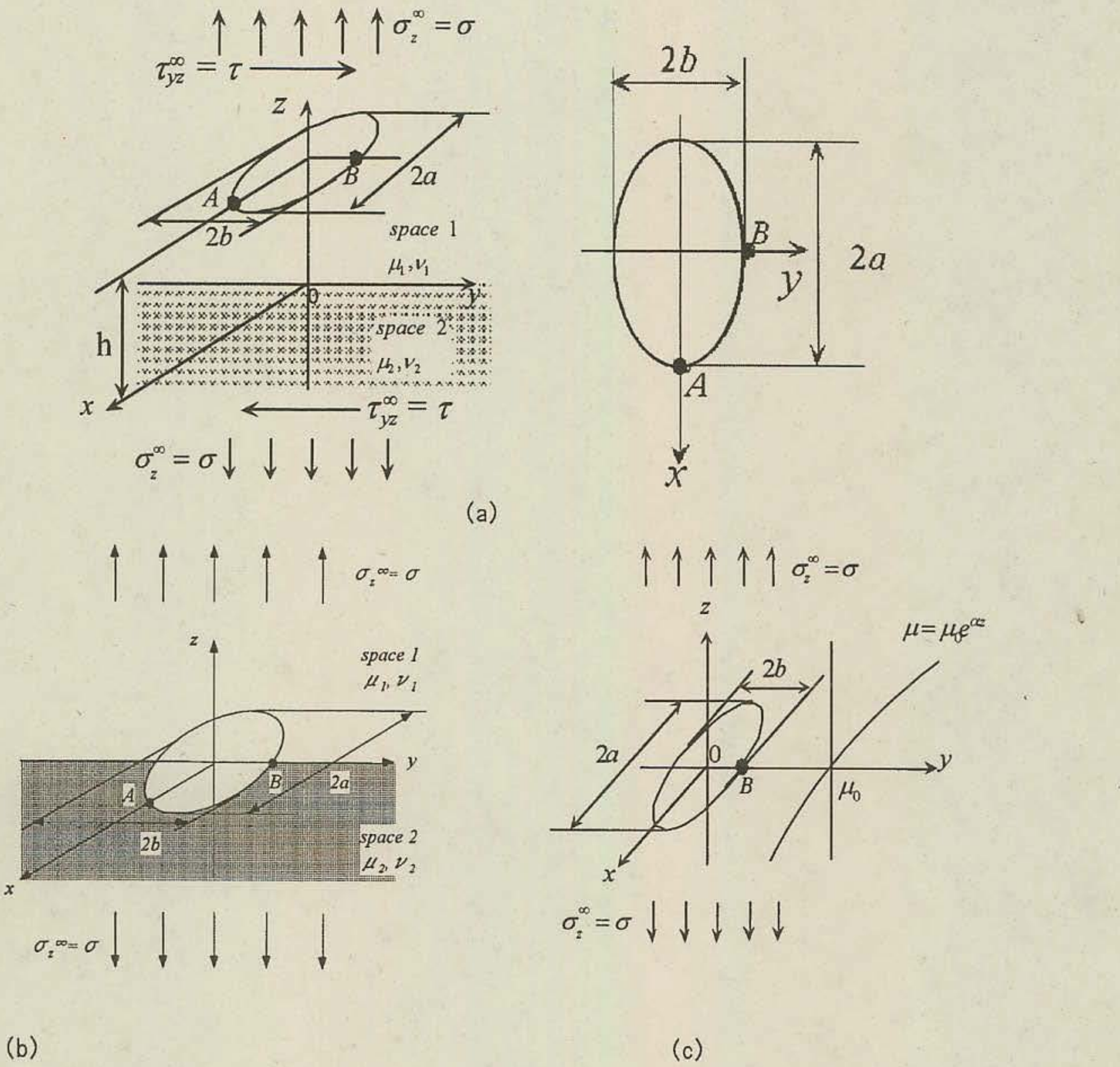

FIG. 2—*Problems considered; (a) an elliptical crack parallel to an interface; (b) an elliptical interface crack; and (c) an elliptical crack in a functionally graded material.*

To confirm the accuracy of the formulas 1–3, the exact maximum stress intensity factors of elliptical [3,4] and rectangular cracks [5,6] at A and B subjected to σ_z^∞ and τ_{yz}^∞ at infinity are shown in Table 1. Here, a, b are dimensions of elliptical and rectangular cracks. It should be noted that F_I^* is independent of Poisson's ratio ν, but F_{II}^*, F_{III}^* are depending on ν. Therefore Table 1 shows the range of the maximum stress intensity factors for $\nu = 0 \sim 0.5$.

In Table 1 it is seen that the maximum stress intensity factors can be calculated effectively by formulas 1–3 for the arbitrary 3-D cracks in homogeneous infinite body.

In recent years, however, since composite materials have been widely used in many industrial fields, the stress intensity evaluation formulas for a crack in the vicinity of an interface become particularly important. In the previous paper [7], therefore, the stress intensity evaluation formulas were proposed for an arbitrary-shaped 3-D crack perpendicular to an interface.

In this paper, the maximum stress intensity factors for a crack

TABLE 1—*Maximum stress intensity factors at A or B for an elliptical crack or rectangular crack in Fig. 1.*

	Stress Intensity Evaluation Formulas	Elliptical Crack	Rectangular Crack
F_{I-n}^* at A	≅0.5, a/b≤1	0.47∼0.52[(3)]	0.47∼0.52[(5)]
F_{I-n}^* at B	≅0.5, a/b≥1	0.47∼0.52[(3)]	0.47∼0.52[(5)]
F_{II-s}^* at B	≅0.55, a/b≥1	0.46∼0.64[(4)]	0.47∼0.64[(6)]
F_{III-s}^* A	≅0.45, a/b≤1	0.32∼0.52[(4)]	0.39∼0.54[(6)]

where $F_I^* = K_{I\max}/\sigma_z^\infty\sqrt{\pi\sqrt{area}}$, $F_{II}^* = K_{II\max}/\tau_{yz}^\infty\sqrt{\pi\sqrt{area}}$, $F_{III}^* = K_{III\max}/\tau_{yz}^\infty\sqrt{\pi\sqrt{area}}$.

TABLE 2—(a) *Effect of Poisson's ratio when $\sigma_z^\infty=\sigma$, $\tau_{yz}^\infty=0$ in Fig. 2(a).* (b) *Effect of Poisson's ratio when $\sigma_z^\infty=0$, $\tau_{yz}^\infty=\tau$ in Fig. 2(a).*

a/b			16						1		
h/2b			0.1			0.4			0.1	0.4	
μ_2/μ_1			0	0.5	∞	0	0.5	∞	0.5	0.5	
	$\nu_1=0.0$	$\nu_2=0.0$	5.9439	1.1524	0.6678	1.7090	1.0857	0.798	0.7243	0.6710	
	$\nu_1=0.5$	$\nu_2=0.5$	5.9443	1.1971	0.7101	1.7092	1.1316	0.760	0.7563	0.6901	
F_{I-n}	$\nu_1=0.0$	$\nu_2=0.5$	5.9439	1.0055	0.6678	1.7090	1.0352	0.798	0.6544	0.6586	
	$\nu_1=0.5$	$\nu_2=0.0$	5.9443	1.3145	0.7101	1.7092	1.1628	0.760	0.8093	0.6971	
	$\nu_1=0.3$	$\nu_2=0.3$	5.9434	1.1748	0.7122	1.7090	1.1073	0.800	0.7397	0.6800	
	$\nu_1=0.0$	$\nu_2=0.0$	3.0239	0.0917	−0.2210	0.288	0.0371	−0.084	0.0513	0.0141	
	$\nu_1=0.5$	$\nu_2=0.5$	3.0220	0.0800	−0.0866	0.287	0.0530	−0.082	0.0507	0.0214	
F_{II-n}	$\nu_1=0.0$	$\nu_2=0.5$	3.0239	−0.0576	−0.2210	0.288	0.0119	−0.084	−0.0201	0.0104	
	$\nu_1=0.5$	$\nu_2=0.0$	3.0220	0.2142	−0.0866	0.287	0.0683	−0.082	0.1074	0.0249	
	$\nu_1=0.3$	$\nu_2=0.3$	3.0228	0.0921	−0.1519	0.287	0.0446	−0.075	0.0520	0.0176	(a)
a/b			16						1		
h/2b			0.1			0.4			0.1	0.4	
μ_2/μ_1			0	0.5	∞	0	0.5	∞	0.5	0.5	
	$\nu_1=0.0$	$\nu_2=0.0$	1.2053	1.0817	0.6944	1.0950	1.0241	0.8540	0.6865	0.6456	
	$\nu_1=0.5$	$\nu_2=0.5$	1.2073	1.0789	0.8240	1.0984	1.0279	0.9277	0.9058	0.8622	
F_{II-s}	$\nu_1=0.0$	$\nu_2=0.5$	1.2053	0.9625	0.6944	1.0950	0.9830	0.8540	0.6727	0.6410	
	$\nu_1=0.5$	$\nu_2=0.0$	1.2073	1.1557	0.8240	1.0984	1.0506	0.9277	0.9252	0.8669	
	$\nu_1=0.3$	$\nu_2=0.3$	1.2085	1.0855	0.7724	1.0994	1.0302	0.9025	0.8040	0.7600	
	$\nu_1=0.0$	$\nu_2=0.0$	−0.0634	−0.0616	−0.0558	−0.0606	−0.0974	−0.0604	−0.6790	−0.6482	
	$\nu_1=0.5$	$\nu_2=0.5$	−0.0325	−0.0313	−0.0289	−0.0306	−0.0306	−0.0307	−0.4456	−0.4342	
F_{III-s}	$\nu_1=0.0$	$\nu_2=0.5$	−0.0634	−0.0597	−0.0558	−0.0606	−0.0604	−0.0604	−0.6299	−0.6414	
	$\nu_1=0.5$	$\nu_2=0.0$	−0.0325	−0.0312	−0.0289	−0.0306	−0.0307	−0.0307	−0.4722	−0.4374	
	$\nu_1=0.3$	$\nu_2=0.3$	−0.0448	−0.0435	−0.0403	−0.0427	−0.0428	−0.0427	−0.5557	−0.5350	(b)

parallel to an interface under σ_z^∞ and τ_{yz}^∞ will be considered. For this problem, the formulas 1–3 can be applied only if the distance between the crack and interface is quite large. Generally, the maximum stress intensity factors will be functions of the distance from crack to the interface h (see Fig. 2(*a*)), and shear modulus ratio μ_2/μ_1. Here the results of an elliptical crack parallel to interface [8] will be used to investigate the maximum stress intensity factors of arbitrary 3-D cracks. These results [8] were accurately obtained by the body force method coupled with singular integral equation formulation. Meanwhile, cracks on the interface, and cracks in functionally graded materials (FGMs) as shown in Fig. 2(*b*) and 2(*c*) will also be considered. Since FGMs have no interface, which may be harmful for the strength of structures, they have attracted wide attention.

In the following discussions, the dimensionless stress intensity factors defined as Eqs 4 and 5 will be used.

$$\left.\begin{aligned} F_{I-n}&=K_{\text{Imax}}/\sigma_z^\infty\sqrt{\pi b}, & F^*_{I-n}&=K_{\text{Imax}}/\sigma_z^\infty\sqrt{\pi\sqrt{area}} \\ F_{II-n}&=K_{\text{IImax}}/\sigma_z^\infty\sqrt{\pi b}, & F^*_{II-n}&=K_{\text{IImax}}/\sigma_z^\infty\sqrt{\pi\sqrt{area}} \\ F_{III-n}&=K_{\text{IIImax}}/\sigma_z^\infty\sqrt{\pi a}, & F^*_{III-n}&=K_{\text{IIImax}}/\sigma_z^\infty\sqrt{\pi\sqrt{area}} \end{aligned}\right\} \quad (4)$$

$$\left.\begin{aligned} F_{I-s}&=K_{\text{Imax}}/\tau_{yz}^\infty\sqrt{\pi b}, & F^*_{I-s}&=K_{\text{Imax}}/\tau_{yz}^\infty\sqrt{\pi\sqrt{area}} \\ F_{II-s}&=K_{\text{IImax}}/\tau_{yz}^\infty\sqrt{\pi b}, & F^*_{II-s}&=K_{\text{IImax}}/\tau_{yz}^\infty\sqrt{\pi\sqrt{area}} \\ F_{III-s}&=K_{\text{IIImax}}/\tau_{yz}^\infty\sqrt{\pi a}, & F^*_{III-s}&=K_{\text{IIImax}}/\tau_{yz}^\infty\sqrt{\pi\sqrt{area}} \end{aligned}\right\} \quad (5)$$

Here, F_{i-n} and F_{i-s} (i=*I*,*II*,*III*) are dimensionless stress intensity factors normalized by two-dimensional solutions, under tension and shear, respectively. On the other hand, F^*_{i-n} and F^*_{i-s} (i=*I*,*II*,*III*) are dimensionless factors normalized by $\sqrt{area}$ parameter, under tension and shear, respectively.

Effect of Poisson's Ratio on the Stress Intensity Factors

If an elliptical crack is close to an interface, the stress intensity factors vary depending on Poisson's ratios of materials 1 and 2. Table 2 shows Mode I stress intensity factor in Fig. 2(*a*). Here, a,b are dimensions of elliptical and rectangular cracks, h is the distance from the crack to the interface (see Fig. 2), and μ_2/μ_1 is shear modulus ratio. The F_{I-n} values vary by about 24 % when $h/2b=0.1$. If we use the results for $\nu_1=\nu_2=0.3$, the stress intensity factor can be evaluated within 12 % even when Poisson's ratios are changed extremely from 0 to 0.5. When the distance between crack and interface is $h/2b=0.4$, the F_{I-n} values vary only by 7 %. Therefore, in the following calculations $\nu_1=\nu_2=0.3$ is simply assumed.

Maximum Stress Intensity Factors of a Crack Parallel an Interface Subjected to Normal Loads

In the previous studies [8], the stress intensity factor in Fig. 2(*a*) was analyzed under $\sigma_z^\infty=\sigma$, $\tau_{yz}^\infty=0$ at infinity; then, $\sqrt{area}$ parameter is found to be effective because the values of F^*_{I-n} are insensitive for the crack shape in most cases. In this paper, therefore, F^*_{I-n} formula is proposed by approximating F^*_{I-n} as a function of μ_2/μ_1 and

TABLE 3—*Dimensionless stress intensity factor F^*_{I-n} at B under tension $\sigma_z^\infty=\sigma$ in Fig. 1(a).*

h/2b	μ_2/μ_1	0.01	0.05	0.1	0.3	1.0
	a/b=1	1.5526	1.0869	0.8826	0.6352	0.4782
0.1	→∞	2.0283	1.2166	0.9444	0.6494	0.4729
	[1]/[∞]	0.7655	0.8934	0.9346	0.9781	1.0112
	a/b=1	0.9372	0.8263	0.7417	0.5953	0.4782
0.2	→∞	1.2656	1.0075	0.8492	0.6249	0.4729
	[1]/[∞]	0.7405	0.8201	0.8734	0.9526	1.0112
	a/b=1	0.7282	0.6854	0.6463	0.5621	0.4782
0.3	→∞	0.9479	0.8401	0.7542	0.5995	0.4729
	[1]/[∞]	0.7682	0.8159	0.8569	0.9376	1.0112
	a/b=1	0.6327	0.6110	0.5895	0.5377	0.4782
0.4	→∞	0.7927	0.7352	0.6836	0.5760	0.4729
	[1]/[∞]	0.7982	0.8311	0.8623	0.9335	1.0112
	a/b=1	0.5808	0.5679	0.5547	0.5209	0.4782
0.5	→∞	0.7040	0.6683	0.6342	0.5564	0.4729
	[1]/[∞]	0.8250	0.8498	0.8746	0.9362	1.0112
	a/b=1	0.5006	0.4982	0.49567	0.4886	0.4782
1.0	→∞	0.5477	0.5391	0.5301	0.5059	0.4729
	[1]/[∞]	0.9140	0.9351	0.9351	0.9657	1.0112
	a/b=1	0.4817	0.4810	0.4810	0.4798	0.4782
2.0	→∞	0.4936	0.4891	0.4891	0.4726	0.4729
	[1]/[∞]	0.9759	0.9833	0.9833	0.9943	1.0112
	a/b=1	0.4782	0.4782	0.4782	0.4782	0.4782
∞	→∞	0.4729	0.4729	0.4729	0.4729	0.4729
	[1]/[∞]	1.0112	1.0112	1.0112	1.0112	1.0112

$h/2b$. Although in Ref. [8], the results for μ_2/μ_1=0,0.5,2, ∞ were given, they are not enough for proposing the formula. Thus, the numerical calculation has been newly performed for μ_2/μ_1 =0.01,0.05, 0.1,0.3,1.0 with varying the distance in the range of $h/2b=0.1\sim\infty$. Then, the results are shown in Tables 3 and 4. In Table 4, it is seen that F^*_{II-n} may be negligible except for the case that the crack is very close to the interface. As shown in Table 3, F^*_{I-n} value is strongly dependent on a/b as $\mu_2/\mu_1\to 0$ and $h/2b$

TABLE 4—*Dimensionless stress intensity factor F^*_{II-n} at B under tension $\sigma_z^\infty=\sigma$ in Fig. 1(a).*

h/2b	μ_1/μ_1	0.01	0.05	0.1	0.3	1.0
	a/b=1	0.6357	0.3380	0.2141	0.0796	0.0000
0.1	→∞	0.9174	0.4067	0.2459	0.0894	0.0000
	[1]/[∞]	0.6929	0.8312	0.8406	0.8909	
	a/b=1	0.2382	0.1774	0.1321	0.0566	0.0000
0.2	→∞	0.4100	0.2690	0.1848	0.0713	0.0000
	[1]/[∞]	0.5809	0.6595	0.7146	0.7934	
	a/b=1	0.1150	0.0947	0.0763	0.0375	0.0000
0.3	→∞	0.2162	0.1653	0.1252	0.0549	0.0000
	[1]/[∞]	0.5319	0.5731	0.6095	0.6821	
	a/b=1	0.0634	0.0543	0.0462	0.0242	0.0000
0.4	→∞	0.1293	0.1055	0.0843	0.0407	0.0000
	[1]/[∞]	0.4902	0.5148	0.5479	0.5938	
	a/b=1	0.0977	0.0329	0.0280	0.0156	0.0000
0.5	→∞	0.0836	0.0705	0.0579	0.0299	0.0000
	[1]/[∞]	0.4512	0.4669	0.4837	0.5231	
	a/b=1	0.0051	0.0045	0.0040	0.0024	0.0000
1.0	→∞	0.0168	0.0149	0.0129	0.0074	0.0000
	[1]/[∞]	0.3020	0.3050	0.3088	0.3747	
	a/b=1	0.0004	0.0004	0.0003	0.0002	0.0000
2.0	→∞	0.0025	0.0023	0.0020	0.0012	0.0000
	[1]/[∞]	0.1700	0.1698	0.1710	0.1716	
	a/b=1	0.0000	0.0000	0.0000	0.0000	0.0000
0.1	→∞	0.0000	0.0000	0.0000	0.0000	0.0000
	[1]/[∞]					

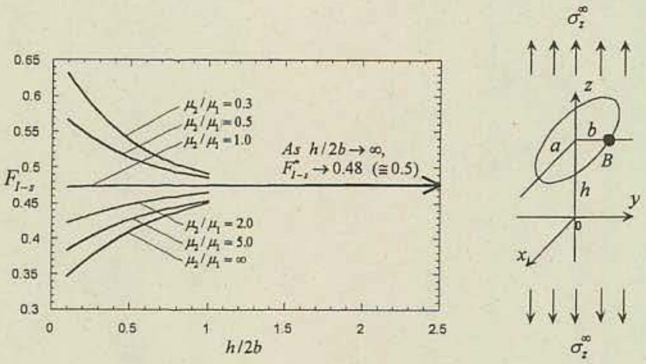

FIG. 3—F^*_{I-n} *values of Eq 5 useful for* $a/b\geq 1$, ($\nu=0.3$).

$\to 0$. For $\mu_2/\mu_1 \geq 0.3$, Eq 6 may be proposed by applying the least square method to the average value of $a/b=1$ and $a/b\to\infty$.

$$\left.\begin{array}{l}
(1)\ \text{When } 0.1 \leq h/2b \leq 1.0,\\
F^*_{I-n} = (0.839 - 0.703G + 0.449G^2 - 0.113G^3)\\
\quad -(0.724 - 1.463G + 0.968G^2 - 0.237G^3)H\\
\quad +(0.504 - 1.048G + 0.709G^2 - 0.172G^3)H^2\\
\quad -(0.117 - 0.246G + 0.169G^2 - 0.041G^3)H^3\\
\text{if } H = h/2b,\\
\begin{cases} 0.3 \leq \mu_2/\mu_1 \leq 1.0 \text{ and } G=\mu_2/\mu_1\\ 1.0 \leq \mu_2/\mu_1 \leq \infty \text{ and } G = 2-\mu_1/\mu_2\end{cases}\\
(2)\ \text{When } h/2b > 1.0,\ F^*_{I-n} = 0.48 (\cong 0.5)
\end{array}\right\} \quad (6)$$

Equation 6 evaluates the maximum stress intensity factor F^*_{I-n} of arbitrary-shaped cracks within about 10 % when $\mu_2/\mu_1 \geq 0.3$ and $h/2b \geq 0.3$. Figure 3 shows the values of Eq 6. Since Eq 6 is based on only the results of $a/b=1$, $a/b\to\infty$, $F^*_{I-n}=0.48$ as $h/2b\to\infty$ instead of $F^*_{I-n}=0.5$.

Maximum Stress Intensity Factors of a Crack Parallel to an Interface Subjected to Shear Loads

The problem in Fig. 2(*a*) under $\sigma_z^\infty=0$, $\tau_{yz}^\infty=\tau$ at infinity can be analyzed in a similar way to Ref. [8]. The maximum stress intensity factors at B and A (F_{II-s}, and F_{III-s}) are shown in Fig. 4 for different value of $h/2b$ when $\mu_2/\mu_1=0,\infty$. On the one hand, Fig. 5 shows the values of the maximum stress intensity factors F^*_{II-s}, F^*_{III-s} normalized by $\sqrt{area}$ parameter when $\mu_2/\mu_1=0,\infty$. It is seen that F^*_{II-s} and F^*_{III-s} are insensitive to the crack shape in comparison with F_{II-s} and F_{III-s}. Consider a ratio of $a/b=1$ to $a/b\to\infty$; then, we found that F_{II-s} varies in the range of $0.7140\sim 0.7991$, whereas F^*_{II-s}, varies in the range $1.130\sim 1.268 \cong 1$ (see Table 5). On the other hand, for a ratio of $a/b=1$ to $a/b=1/16$, the ratio of F_{III-s} varies in the range of $0.4133\sim 0.5708$, whereas F^*_{III-s} varies in the range of $0.6565 \sim 0.9069 \cong 1$ (see Table 6). When $\mu_2/\mu_1\to 0$ and $h/2b\to 0$, F^*_{III-s} becomes sensitive to the crack shape a/b.

Equation 7 is obtained by applying the least square method to the average value of F^*_{II-s} for $a/b=1$ and $a/b\to\infty$. Equation 8 is obtained similarly from the average value of F^*_{III-s} for $a/b=1$ and $a/b=1/16$.

When $0.1 \leq h/2b \leq 1.0$ and $a/b \geq 1$

$$F^*_{II-s} = (0.628 - 0.267H + 0.216H^2 - 0.055H^3) - (0.113 - 0.274H + 0.222H^2 - 0.057H^3)G \quad (7)$$

When $0.1 \leq h/2b \leq 1.0$ and $a/b \leq 1$

$$\left.\begin{array}{l}
F^*_{III-s} = -(0.697 - 0.607G + 0.438G^2 - 0.114G^3)\\
\quad -(1.016 - 2.465G + 1.829G^2 - 0.462G^3)H\\
\quad -(1.437 - 3.635G + 2.751G^2 - 0.689G^3)H^2\\
\quad +(0.848 - 2.203G + 1.693G^2 - 0.424G^3)H^3\\
\quad -(0.175 - 0.463G + 0.359G^2 - 0.903G^3)H^4
\end{array}\right\} \quad (8)$$

Here $H=h/2b$ and

$$\begin{cases} 0.0 \leq \mu_2/\mu_1 \leq 1.0, & G=\mu_2/\mu_1\\ 1.0 \leq \mu_2/\mu_1 \leq \infty, & G=2-\mu_1/\mu_2\end{cases}$$

When $h/2b \geq 1.0$ and $a/b \geq 1$ $F^*_{II}=0.52(\cong 0.55)$
When $h/2b \geq 1.0$ and $a/b \leq 1$ $F^*_{III}=0.43(\cong 0.45)$

Equation 7 gives F^*_{II-s} values of an arbitrary crack within 13 % error, and Eq 8 gives F^*_{III-s} values within 17 % error. Figures 6 and 7 show the values given by formulas 7 and 8. When $h/2b\to\infty$ the results go to $F^*_{II-s}=0.52$ ($\cong 0.55$, see Eq 2), and $F^*_{III-s}=0.43$ ($\cong 0.45$, see Eq 3). The difference comes from the results used for Eqs 7 and 8 are limited to the case of $\nu_1=\nu_2=0.3$. As shown in Figs. 4 and 5, the values of F^*_{I-s} under shear loads τ_{yz}^∞ can be neglected except for the case of the crack very close to the interface.

Maximum Stress Intensity Factor for an Interface Crack

For interface cracks as $h\to 0$ in Fig. 2(*a*), the maximum stress intensity factors K_1 and K_2 at point B are defined as follows:

$$\sigma_z + i\tau_{rz} \to \frac{K_1 + iK_2}{\sqrt{2\pi r}}\left(\frac{r}{2a}\right)^{i\varepsilon}, \quad (r=y-b\to 0) \quad (9)$$

where

$$\varepsilon = \frac{1}{2\pi}\ln\left[\frac{\kappa_1}{\mu_1}+\frac{1}{\mu_2}\right]\bigg/\left[\frac{\kappa_2}{\mu_2}+\frac{1}{\mu_1}\right]$$

$$\kappa_j = 3-4\nu_j, \quad (j=1,2) \quad (10)$$

is seen that $\sqrt{area}$ parameter is useful for evaluating the interface crack (Table 7). In Section 3, it is seen that the F^*_{I-n} value of the parallel crack is dependent on the crack shape when $\mu_2/\mu_1<0.3$ and $h/2b\to 0$. However, for interface cracks, the $\sqrt{area}$ parameters are found to be more effective because the ratio of the results of $a/b=1$ to $a/b\to\infty$ is in the range $0.996\sim 1.011\cong 1.0$.

Maximum Stress Intensity Factor for a Crack in FGMs

Cracks in functionally graded materials (FGMs) were widely studied by Erdogan and other researchers [11–13]. However, since those studies were limited to two-dimensional or axisymmetric solutions in most cases, it is desirable to evaluate three-dimensional cracks in FGMs. Here the stress intensity factors are considered in

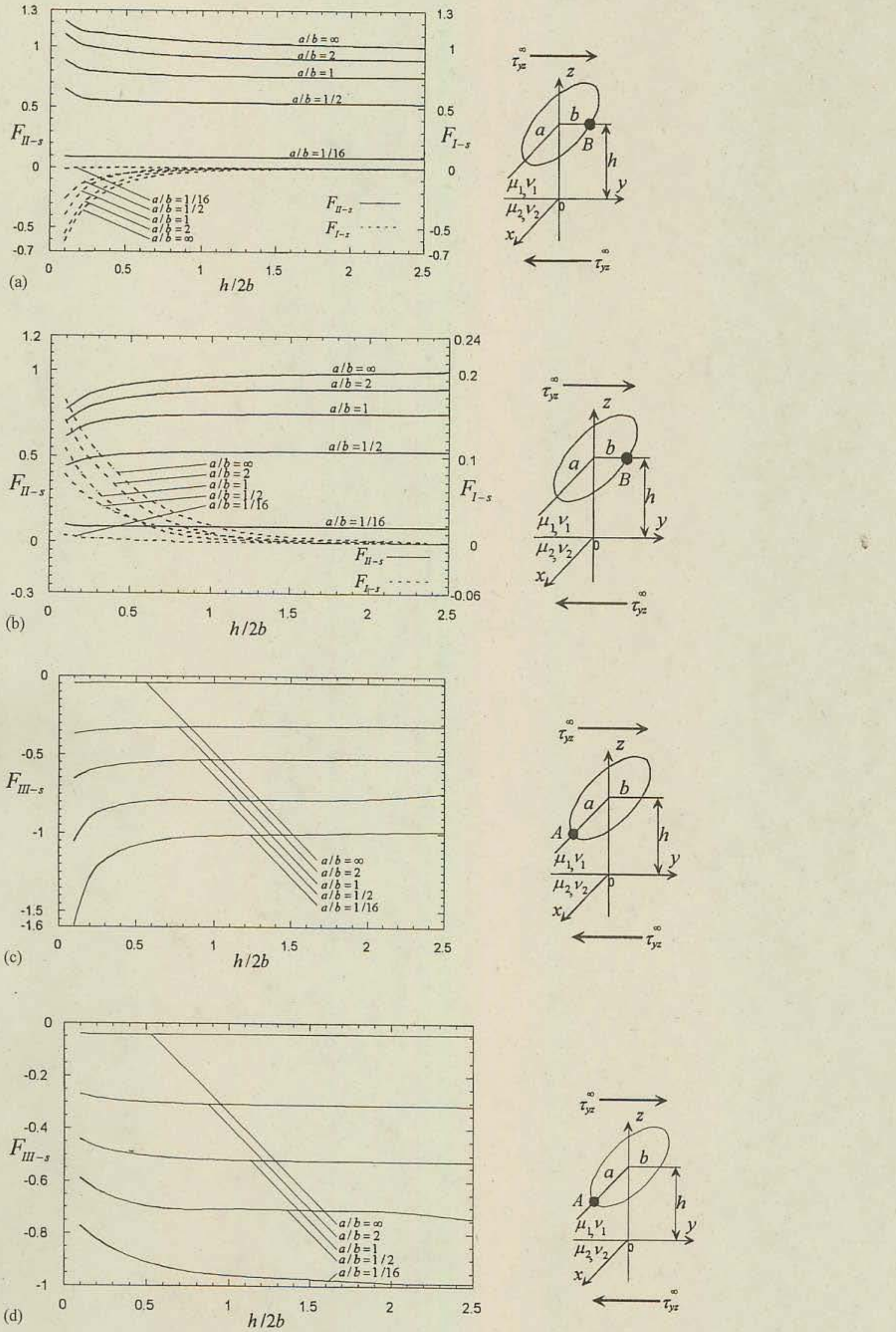

FIG. 4—(a) *Variation of* F_{I-s}, F_{II-s} *at B when* $\mu_2/\mu_1=0$, $\nu_1,\nu_2=0.3$ *under shear* $\tau_{yz}^{\infty}=\tau$ *in Fig. 2(a).* (b) *Variation of* F_{I-s}, F_{II-s} *at B when* $\mu_2/\mu_1=\infty$, $\nu_1,\nu_2=0.3$ *under shear* $\tau_{yz}^{\infty}=\tau$ *in Fig. 2(a).* (c) *Variation of* F_{III-s} *at A when* $\mu_2/\mu_1=0$, $\nu_1,\nu_2=0.3$ *under shear* $\tau_{yz}^{\infty}=\tau$ *in Fig. 2(a).* (d) *Variation of* F_{III-s} *at A when* $\mu_2/\mu_1=\infty$, $\nu_1,\nu_2=0.3$ *under shear* $\tau_{yz}^{\infty}=\tau$ *in Fig. 2(a).*

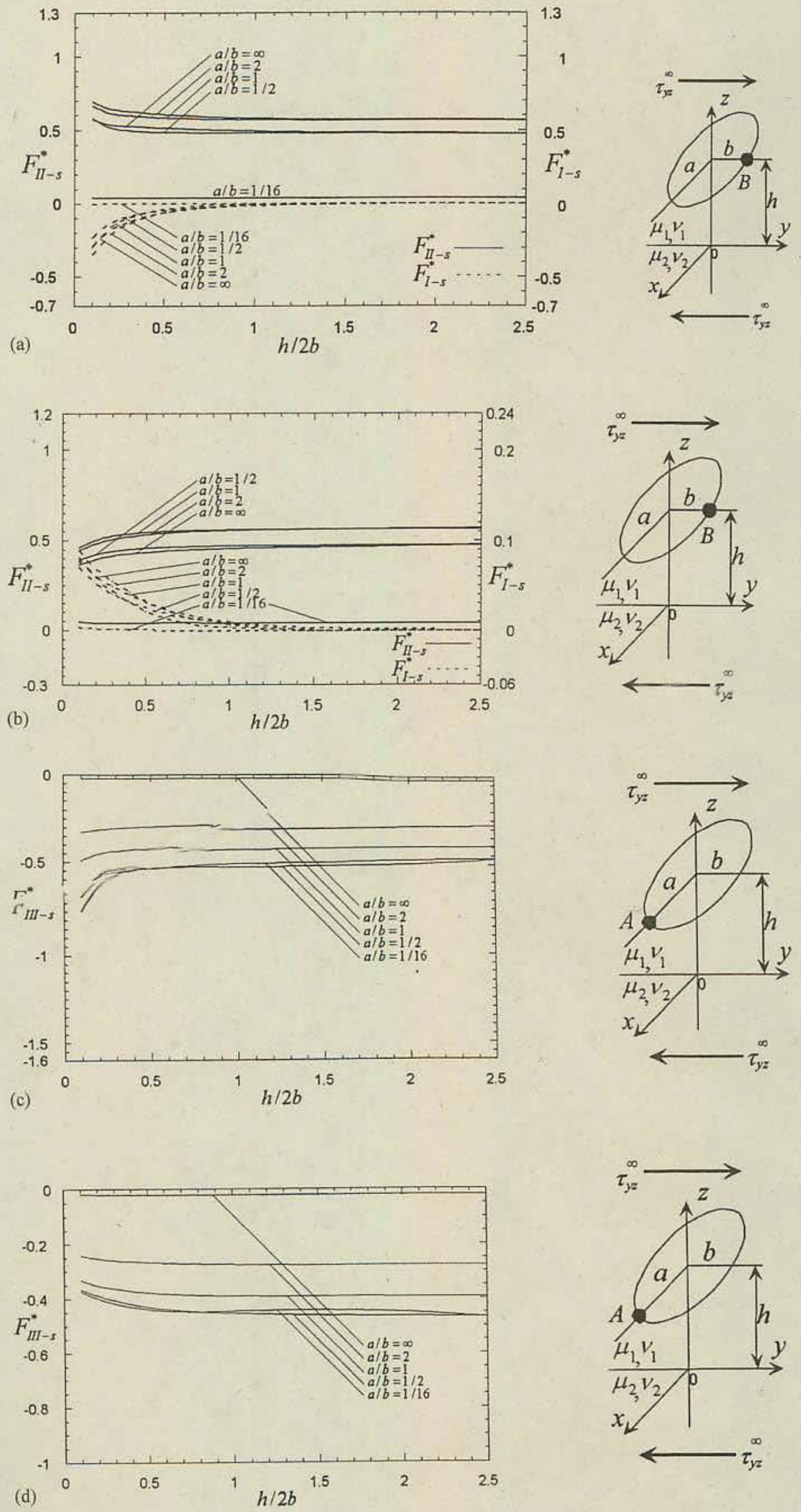

FIG. 5—(a) *Variation of* F^*_{I-s}, F^*_{II-s} *at B when* $\mu_2/\mu_1=0$, $\nu_1,\nu_2=0.3$ *under shear* $\tau^{\infty}_{yz}=\tau$ *in Fig. 2(a).* (b) *Variation of* F^*_{I-s}, F^*_{II-s} *at B when* $\mu_2/\mu_1=\infty$, $\nu_1,\nu_2=0.3$ *under shear* $\tau^{\infty}_{yz}=\tau$ *in Fig. 2(a).* (c) *Variation of* F^*_{III-s} *at A when* $\mu_2/\mu_1=0$, $\nu_1,\nu_2=0.3$ *under shear* $\tau^{\infty}_{yz}=\tau$ *in Fig. 2(a).* (d) *Variation of* F^*_{III-s} *at A when* $\mu_2/\mu_1=\infty$, $\nu_1,\nu_2=0.3$ *under shear* $\tau^{\infty}_{yz}=\tau$ *in Fig. 2(a).*

TABLE 5—*Dimensionless stress intensity factor F_{II-s}, F^*_{II-s} at B under shear $\tau^{\infty}_{yz}=\tau$ in Fig. 2(a).*

		F_{II-s}				F^*_{II-s}			
$h/2b$	a/b	$\mu_2/\mu_1=0$	$\mu_2/\mu_1=0.5$	$\mu_2/\mu_1=2.0$	$\mu_2/\mu_1=\infty$	$\mu_2/\mu_1=0$	$\mu_2/\mu_1=0.5$	$\mu_2/\mu_1=0.2$	$\mu_2/\mu_1=\infty$
0.1	1/16	0.091	0.089	0.085	0.098	0.0428	0.0471	0.0402	0.0463
	1/2	0.647	0.571	0.496	0.440	0.5779	0.5103	0.4428	0.3929
	1	0.8827	0.8040	0.6995	0.6131	0.6630	0.6036	0.5254	0.4605
	2	1.098	0.9745	0.8256	0.7026	0.6935	0.6155	0.5215	0.4438
	$\to\infty$	1.2085	1.0855	0.9210	0.7724	0.5715	0.5133	0.4355	0.3652
	$(a/b=1)/(a/b=\infty)$	0.7304	0.7407	0.7595	0.7938	1.1601	1.1765	1.2064	1.2610
0.2	1/16	0.0870	0.0870	0.0863	0.0858	0.0411	0.0411	0.0408	0.0405
	1/2	0.5777	0.5508	0.5108	0.4746	0.5160	0.4920	0.4560	0.4238
	1	0.8161	0.7750	0.7228	0.6700	0.6130	0.5821	0.5429	0.5033
	2	1.018	0.9402	0.8518	0.7649	0.6430	0.5938	0.5380	0.4831
	$\to\infty$	1.1330	1.0501	0.9484	0.8384	0.5358	0.4966	0.4485	0.3965
	$(a/b=1)/(a/b=\infty)$	0.7203	0.7380	0.7621	0.7991	1.1441	1.1722	1.2105	1.2694
0.5	1/16	0.0863	0.0865	0.0865	0.0868	0.0408	0.0409	0.0409	0.0410
	1/2	0.5430	0.5355	0.5249	0.5125	0.4851	0.4781	0.4687	0.4579
	1	0.7574	0.7573	0.7409	0.7243	0.5831	0.5688	0.5565	0.5440
	2	0.9175	0.9142	0.8780	0.8423	0.6054	0.5774	0.5546	0.5320
	$\to\infty$	1.0433	1.0259	0.9745	0.9188	0.5142	0.4851	0.4608	0.4345
	$(a/b=1)/(a/b=\infty)$	0.7140	0.7382	0.7603	0.7883	1.1340	1.1725	1.2077	1.2520
2.0	1/16	0.0865	0.0865	0.0865	0.0868	0.0409	0.0409	0.0409	0.0410
	1/2	0.5325	0.5310	0.5298	0.5287	0.4757	0.4744	0.4733	0.4723
	1	0.7505	0.7494	0.7486	0.7478	0.5637	0.5624	0.5608	0.5617
	2	0.8998	0.8966	0.8946	0.8925	0.5683	0.5665	0.5650	0.5637
	$\to\infty$	1.0141	1.0141	0.9960	0.9878	0.4735	0.4748	0.4671	0.4671
	$(a/b=1)/(a/b=\infty)$	0.7400	0.7463	0.7516	0.7714	1.1755	1.1855	1.1938	1.2026
∞	1/16	0.0865	0.0865	0.0865	0.0865	0.0409	0.0409	0.0409	0.0409
	1/2	0.5304	0.5304	0.5304	0.5304	0.4768	0.4768	0.4768	0.4768
	1	0.7491	0.7491	0.7491	0.7491	0.5627	0.5627	0.5627	0.5627
	2	0.8957	0.8957	0.8957	0.8957	0.5657	0.5657	0.5657	0.5657
	$\to\infty$	1.0000	1.0000	1.0000	1.0000	0.4729	0.4729	0.4729	0.4729
	$(a/b=1)/(a/b=\infty)$	0.7491	0.7491	0.7491	0.7491	0.1299	1.1299	1.1299	1.1299

terms of $\sqrt{area}$ parameter for $a/b=1$, $a/b\to\infty$ in Fig. 2(*b*). Table 8 shows the results for $a/b=1,\infty$ with the ratio of the results of $(a/b=1)/(a/b=\infty)$. Here the notation α is used as a nonhomogeneity parameter for functionally graded materials and a is a dimension of a crack in FGM. Then, the SIF is controlled by αa. As shown in Table 8, the ratio of F_I is within $0.637\sim0.462$, and the ratio of F^*_I is within $0.99\sim1.36$. Since the value of F^*_I is insensitive to a/b, $\sqrt{area}$ parameter is found to be useful for evaluating the results for elliptical cracks from two-dimensional solutions available for FGMs [13].

Conclusions

In this study, stress intensity factors of three-dimensional cracks in the vicinity of an interface were considered with varying the geometrical conditions and elastic modulus ratio μ_2/μ_1. The conclusions can be made in the following way.

(1) For a parallel crack to an interface under tension (see Fig. 2(*a*)), the maximum stress intensity factor F^*_I normalized by $\sqrt{area}$ parameter is insensitive to the crack aspect ratio except for smaller μ_2/μ_1. Then, a stress intensity evaluation formula 6 was proposed as a function of $h/2b$ and μ_2/μ_1.

(2) For a parallel crack to an interface under shear (see Fig. 2(*a*)), the maximum stress intensity factors F^*_{II} and F^*_{III} normalized by $\sqrt{area}$ parameter are insensitive to the crack aspect ratio. Then, stress intensity evaluation formulas 7 and 8 were proposed as functions of $h/2b$ and μ_2/μ_1, which is valid for $\mu_2/\mu_1\geqslant0.3$.

(3) The formulas 6–8 may be useful for the range $\mu_2/\mu_1\geqslant0.3$ and $h/2b\geqslant0.1$. Then, the error may be estimated within ±12 % for the variation of Poisson's ratio, and within ±10 % $\sim\pm17$ % for the variation of crack shape. If the approximated formula is derived as a function of Poisson's ratio or aspect ratio, the accuracy and application range may be improved. The formulas 6–8 were proposed only for the major stress intensity factors. Other minor stress intensity factors may be given in a similar way.

(4) When $\mu_2/\mu_1<0.3$ and $h/2b\to0$, F^*_I of a parallel crack becomes dependent on the crack shape. However, if the results of an interface crack are expressed by using $\sqrt{area}$ parameter, the ratio for $a/b=1$ to $a/b=\infty$ is in the range of $0.996\sim1.011\cong1.0$. Therefore, for an interface crack, $\sqrt{area}$ parameter is more useful (see Table 7).

(5) To evaluate three-dimensional cracks in functionally graded materials, the effectiveness of $\sqrt{area}$ parameter is presented. From two-dimensional solutions available for FGM, three-dimensional cracks may be evaluated by using $\sqrt{area}$ parameter.

TABLE 6—*Dimensionless stress intensity factor F_{III-s}, F^*_{III-s} at A under shear $\tau^\infty_{yz}=\tau$ in Fig. 1(a).*

		F_{II-s}				F^*_{III-s}			
h/2b	a/b	$\mu_2/\mu_1=0$	$\mu_2/\mu_1=0.5$	$\mu_2/\mu_1=2.0$	$\mu_2/\mu_1=\infty$	$\mu_2/\mu_1=0$	$\mu_2/\mu_1=0.5$	$\mu_2/\mu_1=2.0$	$\mu_2/\mu_1=\infty$
0.1	1/16	−1.579	−1.109	−0.8986	−0.7738	−0.7467	−0.5244	−0.4249	−0.3659
	1/2	−1.052	−0.8150	−0.6841	−0.5899	−0.6645	−0.5148	−0.4321	−0.3726
	1	−0.6526	−0.5557	−0.4955	−0.4413	−0.4902	−0.4174	−0.3722	−0.3315
	2	−0.3676	−0.3274	−0.2996	−0.2705	−0.3284	−0.2924	−0.2676	−0.2417
	$\to\infty$	−0.0448	−0.0435	−0.0420	−0.0403	−0.0212	−0.0206	−0.0199	−0.0190
	$(a/b=1)/(a/b=1/16)$	0.4133	0.5011	0.5514	0.5703	0.6565	0.7960	0.8760	0.9060
0.2	1/16	−1.287	−1.066	−0.9233	−0.8220	−0.6086	−0.5041	−0.4366	−0.3887
	1/2	−0.9048	−0.7856	−0.7042	−0.6332	−0.5715	−0.4962	−0.4448	−0.3999
	1	−0.6033	−0.5443	−0.5057	−0.4693	−0.4532	−0.4088	−0.3798	−0.3525
	2	−0.3509	−0.3232	−0.3041	−0.2842	−0.3134	−0.2886	−0.2716	−0.2538
	$\to\infty$	−0.0433	−0.0429	−0.0426	−0.0421	−0.0205	−0.0203	−0.0201	−0.0199
	$(a/b=1)/(a/b=1/16)$	0.4688	0.5106	0.5477	0.5709	0.7447	0.8110	0.8699	0.9069
0.5	1/16	−1.079	−1.016	−0.9607	−0.9103	−0.5102	−0.4804	−0.4543	−0.4305
	1/2	−0.8033	−0.7599	−0.7270	−0.6957	−0.5074	−0.4800	−0.4592	−0.4394
	1	−0.5523	−0.5321	−0.5169	−0.5028	−0.4148	−0.3997	−0.3883	−0.3777
	2	−0.3309	−0.3183	−0.3088	−0.2995	−0.2956	−0.2843	−0.2758	−0.2676
	$\to\infty$	−0.0428	−0.0428	−0.0428	−0.0427	−0.0202	−0.0202	−0.0202	−0.0202
	$(a/b=1)/(a/b=1/16)$	0.5119	0.5237	0.5380	0.5523	0.8130	0.8320	0.8547	0.8774
2.0	1/16	−0.9955	−0.9904	−0.9851	−0.9851	−0.4707	−0.4683	−0.4658	−0.4658
	1/2	−0.7805	−0.7537	−0.7329	−0.7131	−0.4929	−0.4760	−0.4629	−0.4504
	1	−0.5253	−0.5245	−0.5239	−0.5234	−0.3946	−0.3910	−0.3935	−0.3931
	2	−0.3147	−0.3137	−0.3130	−0.3123	−0.2811	−0.2803	−0.2796	−0.2790
	$\to\infty$	−0.0429	−0.0428	−0.0428	−0.0427	−0.0203	−0.0202	−0.0202	−0.0202
	$(a/b=1)/(a/b=1/16)$	0.5277	0.5296	0.5318	0.5313	0.8382	0.8412	0.8448	0.8439
∞	1/16	−0.9878	−0.9878	−0.9878	−0.9878	−0.4671	−0.4671	−0.4671	−0.4671
	1/2	−0.7429	−0.7429	−0.7429	−0.7429	−0.4692	−0.4692	−0.4692	−0.4692
	1	−0.5243	−0.5243	−0.5243	−0.5243	−0.3938	−0.3938	−0.3938	−0.3938
	2	−0.3134	−0.3134	−0.3134	−0.3134	−0.2799	−0.2799	−0.2799	−0.2799
	$\to\infty$	−0.0428	−0.0428	−0.0428	−0.0428	−0.0202	−0.0202	−0.0202	−0.0202
	$(a/b=1)/(a/b=1/16)$	0.5308	0.5308	0.5308	0.5308	0.8431	0.8431	0.8431	0.8431

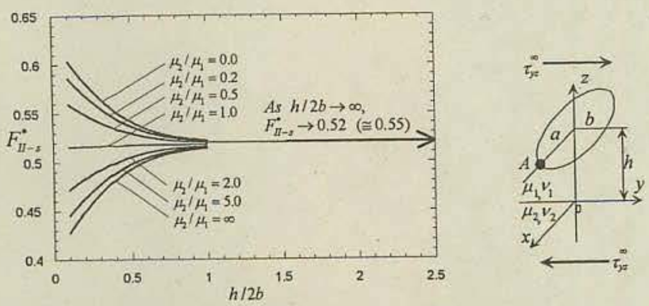

FIG. 6—*Values of Eq 8 useful for $a/b \geq 1$, ($\nu=0.3$).*

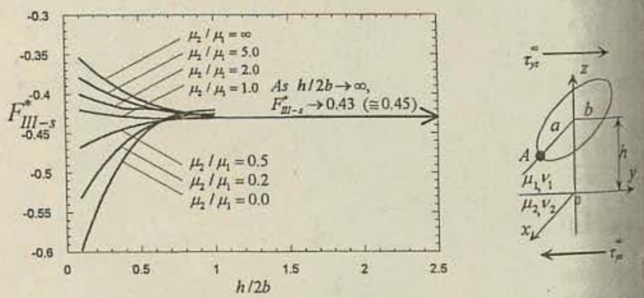

FIG. 7—*Values of Eq 9 useful for $a/b \leq 1$, ($\nu=0.3$).*

TABLE 7—*Interface cracks under tension in Fig. 2(b).*

ε		0.00	0.07	0.15
$\dfrac{K_1}{\sigma\sqrt{\pi b}}$	a/b=1	0.637	0.634	0.627
	→∞	1.000	1.000	1.000
	(a/b=1)/(a/b=∞)	0.637	0.634	0.627
$\dfrac{K_2}{\sigma\sqrt{\pi b}}$	a/b=1	0.000	0.106	0.228
	→∞	0.000	0.140	0.300
	(a/b=1)/(a/b=∞)		0.757	0.760
$\dfrac{K_1}{\sigma\sqrt{\pi\sqrt{area}}}$	a/b=1	0.478	0.476	0.471
	→∞	0.473	0.473	0.473
	(a/b=1)/(a/b=∞)	1.011	1.006	0.996
$\dfrac{K_2}{\sigma\sqrt{\pi\sqrt{area}}}$	a/b=1	0.000	0.080	0.171
	→∞	0.000	0.066	0.142
	(a/b=1)/(a/b=∞)		1.202	1.207

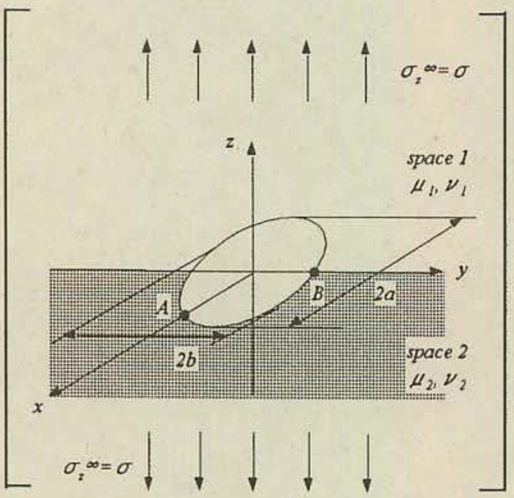

TABLE 8—*Dimensionless stress intensity factor* F_{I-n}, F^{*}_{I-n}, F_{II-n}, F^{*}_{II-n} *at B in Fig. 2(b).*

	αa	0.0	0.1	0.25	0.5	1.0	2.5	5.0
F_{I-n}	a/b=1	0.637	0.638	0.644	0.661	0.712	0.918	1.326
	→∞	1.000	1.008	1.036	1.101	1.258	1.808	2.869
	((a/b=1)/(a/b=∞))	0.637	0.633	0.622	0.600	0.566	0.508	0.462
F_{II-n}	a/b=1	0.000	0.026	0.065	0.129	0.263	0.697	1.567
	→∞	0.000	0.011	0.026	0.053	0.107	0.280	0.611
	((a/b=1)/(a/b=∞))		2.364	2.500	2.434	2.458	2.489	2.565
F^{*}_{I-n}	a/b=1	0.479	0.479	0.484	0.497	0.535	0.690	0.996
	→∞	0.473	0.477	0.490	0.521	0.595	0.855	1.357
	((a/b=1)/(a/b=∞))	1.013	1.004	0.988	0.954	0.899	0.807	0.734
F^{*}_{II-n}	a/b=1	0.000	0.012	0.031	0.061	0.124	0.330	0.741
	→∞	0.000	0.008	0.120	0.040	0.080	0.210	0.459
	((a/b=1)/(a/b=∞))		1.482	1.574	1.533	1.547	1.567	1.615

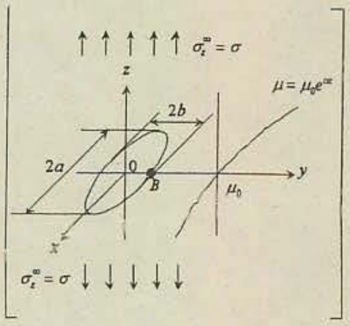

References

[1] Murakami, Y., and Nemat-Nasser, S., "Growth and Stability of Surface Flaws of Arbitrary Shape," *Eng. Fract. Mech.*, Vol. 17, No. 3, 1983, pp. 193–210.

[2] Murakami, Y., "Analysis of Stress Intensity Factors of Modes I, II, and III for Inclined Surface Cracks of Arbitrary Shape," *Eng. Fract. Mech.*, Vol. 22, No. 1, 1985, pp. 101–114.

[3] Irwin, G. R., "Crack Extension Force for a Part-through Crack," *Trans. ASME, J. Appl. Mech.*, Vol. 29, No. 651, 1962, pp. 651–654.

[4] Kassir, M. K., and Sih, G. C., "Three-dimensional Stress Distribution Around an Elliptical Crack Under Arbitrary Loadings," *Trans. ASME, J. Appl. Mech.*, Vol. 33, 1966, pp. 601–611.

[5] Wang, Q., Noda, N.-A., Honda, M.-A., and Chen, M.-C., "Variation of Stress Intensity Factor Along the Front of a 3D Rectangular Crack by Using a Singular Integral Equation Method," *Int. J. Fract.*, Vol. 108, 2001, pp. 119–131.

[6] Noda, N.-A., and Kihara, T.-A., "Variation of the Stress Intensity Factor Along the Front of a 3-D Rectangular Crack Subjected to Mixed-mode Load," *Archive of Applied Mechanics*, Vol. 72, 2002, pp. 599–614.

[7] Noda, N.-A., "Stress Intensity Formulas for Three-dimensional Cracks in Homogeneous and Bonded Dissimilar Materials," *Eng. Fract. Mech.*, Vol. 71, 2004, pp. 1–15.

[8] Noda, N.-A., Ohzono, R., and Chen, M.-C., "Analysis of an Elliptical Crack Parallel to a Bimaterial Interface Under Tension," *Mechanics of Materials*, Vol. 35, 2003, pp. 1059–1076.

[9] Salganik, R. L., "The Brittle Fracture of Cemented Bodies," *Prikl. Mat. Mech.*, Vol. 27, 1963, pp. 400–402.

[10] Kassir, M. K., and Bregman, A. M., "The Stress Intensity Factor for a Penny-shaped Crack Between Two Dissimilar Materials," *Trans. ASME, J. Appl. Mech.*, Vol. 39, 1972, pp. 308–310.

[11] Erdogan, F., and Ozturk, M., "The Axisymmetric Crack Problem in a Nonhomogeneous Medium," *Trans. ASME, J. Appl. Mech.*, Vol. 60, 1993, pp. 406–413.

[12] Konda, N., and Erdogan, F., "Mixed Mode Crack Problem in a Nonhomogeneous Elastic Medium," *Eng. Fract. Mech.*, Vol. 47, 1994, pp. 533–545.

[13] Murakami, Y., Ed., *Stress Intensity Factors Handbook*, The Society of Material Science, Japan, Elsevier, Vol. 5, pp. 1879–2024.